
Improved Outcome Prediction by SPECT Myocardial Perfusion Imaging After CT Attenuation Correction

Aju P. Pazhenkottil*, Jelena-Rima Ghadri*, Rene N. Nkoulou, Mathias Wolfrum, Ronny R. Buechel, Silke M. Küest, Lars Husmann, Bernhard A. Herzog, Oliver Gaemperli, and Philipp A. Kaufmann

Cardiac Imaging, University Hospital Zurich, Zurich, Switzerland

The aim of this study was to determine the impact of attenuation correction with CT (CT-AC) on the prognostic value of SPECT myocardial perfusion imaging (SPECT MPI). **Methods:** The summed stress score (SSS; 20-segment model) was obtained from filtered backprojection (FBP) and iterative reconstruction with CT-AC in 876 consecutive patients undergoing a 1-d stress-rest ^{99m}Tc-tetrofosmin SPECT MPI study for the evaluation of known or suspected coronary artery disease. Survival free of major adverse cardiac events (MACEs; cardiac death or nonfatal myocardial infarction) and survival free of any adverse cardiac events (including cardiac hospitalization, unstable angina, and late coronary revascularization) were analyzed by Kaplan–Meier analysis. **Results:** At a mean follow-up of 2.3 ± 0.6 y, a total of 184 adverse events occurred in 145 patients, including 35 MACEs (16 cardiac deaths [rate, 1.8%] and 19 nonfatal myocardial infarctions [rate, 2.2%]). With FBP, an SSS of 0–3 best distinguished patients with a low MACE rate (0.6%), followed by an SSS of 4–8 (4.3%), with increased MACE rate, and an SSS of 9–13 (3.8%), which was comparable. By contrast, with CT-AC the discrimination of low from intermediate MACE rate was best observed between an SSS of 0 (0%) and an SSS of 1–3 (3.7%), with a plateau at an SSS of 4–8 (3.2%). **Conclusion:** CT-AC for SPECT MPI allows improved risk stratification. The prognostically relevant SSS cutoff is shifted toward lower values.

Key Words: CT-attenuation correction; single-photon emission computed tomography; myocardial perfusion imaging; major adverse cardiac events; outcome

J Nucl Med 2011; 52:196–200

DOI: 10.2967/jnumed.110.080580

SPECT myocardial perfusion imaging (SPECT MPI) is a widely used and well-established method for the evaluation of known or suspected coronary artery disease (CAD). Several studies have shown the strong prognostic value of SPECT MPI (1–3). Nevertheless, attenuation artifacts have remained an important issue. Common sources of artifacts

in MPI studies are soft-tissue attenuation and prominent subdiaphragmatic gastrointestinal activity. To overcome these problems and to better discriminate perfusion defects from artifacts, several methods have been proposed such as integrating findings from gated SPECT (4,5), scanning patients in the prone position (6), and using an external source of irradiation, either a line source (7) or CT (8,9). Attenuation correction (AC) by CT (CT-AC) has been shown to improve image quality and diagnostic accuracy (8–12). CT-AC proved superior to prone MPI acquisition (13) and has several advantages over external radionuclide sources for AC, such as higher photon flux and hence no influence by cross-talk from the SPECT radionuclide, no decay of transmission source, and shorter scan times (14,15). The American Society of Nuclear Cardiology and the Society of Nuclear Medicine have jointly recommended the use of AC in addition to electrocardiography (ECG) gating for SPECT MPI studies (16). The use of CT-AC is likely to increase soon because of the widespread availability of multislice CT scanners. This is particularly true with the integration of the multislice scanners into hybrid SPECT/CT scanners because the low-dose multislice CT images for AC can also be used for coronary calcium scoring (8,17). Although the use of AC in SPECT MPI is emerging and there is evidence of superiority in diagnostic confidence and accuracy of AC over noncorrected SPECT MPI (9,10,12), prognostic SPECT MPI studies using CT-AC are lacking. Thus, the aim of this study was to evaluate the impact of CT-AC on the prognostic value of SPECT MPI.

MATERIALS AND METHODS

Study Population

Consecutive patients who underwent a 1-d adenosine stress-rest ^{99m}Tc-tetrofosmin SPECT MPI study between May 2005 and June 2008 at the Cardiac Imaging Service of the University Hospital Zurich (Switzerland) for the evaluation of known or suspected CAD, with follow-up information available in our clinical database, were identified (*n* = 930). Additional information was gathered from the registry of government authorities in the case of death. Of these, 54 patients were revascularized in the first 30 d after nuclear testing and therefore excluded from further analysis, because during this period any revascularization could potentially be directly triggered by the MPI test result, which would introduce a confounder between diagnostic and prognostic values. Thus, the

Received Jun. 28, 2010; revision accepted Nov. 18, 2010.

For correspondence or reprints contact: Philipp A. Kaufmann, Cardiac Imaging, University Hospital Zurich, Ramistrasse 100, CH-8091 Zurich, Switzerland.

E-mail: pak@usz.ch

*Contributed equally to this work.

COPYRIGHT © 2011 by the Society of Nuclear Medicine, Inc.

prognostic data presented here are based on a subset of 876 patients.

SPECT MPI Image Acquisition and Reconstruction

In all patients, a weight-adjusted dose of 300–400 MBq of ^{99m}Tc -tetrofosmin was injected 3 min into the adenosine infusion (0.14 mg/kg/min). After a delay of 45–60 min, the ECG-gated stress images were acquired. Then, a 3-fold-higher dose of ^{99m}Tc -tetrofosmin was administered, followed by a delay of 45–60 min before acquisition of the ECG-gated rest data. The SPECT MPI acquisition was performed on a dual-head camera (Infinia [until 2006] and Ventri [from 2006 to 2008]; GE Healthcare) with a low-energy, high-resolution collimator; a 20% symmetric window at 140 keV; a 64×64 matrix; and an elliptic orbit with step-and-shoot acquisition at 3° intervals over a 180° arc (45° right anterior oblique to 45° left posterior oblique) with 30 steps (60 views). Scan time was set to 25 s per frame for stress and rest, resulting in a total acquisition time of 14 min 52 s (including interstep rotation time) for each scan, as recommended by the American Society of Nuclear Cardiology (18). Gating included 16 frames per R-R cycle.

For AC, all patients underwent low-dose CT performed using either a Hawkeye system (Infinia; GE Healthcare [until 2006]; 140 kV, 3.0 mA, with a single slice being imaged in about 14 s) or a Light Speed VCT scanner (GE Healthcare [since 2006]; 120 kV and 200–250 mA, depending on the patient's size) during breath-hold as previously reported (8). After reconstruction and transfer to a Xeleris workstation (GE Healthcare), AC maps were generated as previously reported in detail (8,17). SPECT images were reconstructed into short and vertical and horizontal long axes using standard reconstruction—that is, filtered backprojection (FBP)—and iterative reconstruction with CT-AC (Fig. 1). The data were thereafter quantitatively analyzed on the commercially available QPS/QGS software (Cedars-Sinai Medical Center) (19).

Data Analysis

A 20-segment model was used to determine percentage uptake of the radionuclide (18). The following scale was used to stratify percentage uptake in each segment (20): more than 70%, normal (score, 0); 50%–69%, mildly reduced (score, 1); 30%–49%, moderately reduced (score, 2); 10%–29%, severely reduced (score, 3); and less than 10% absent (score, 4). A summed stress score (SSS) was obtained by adding the scores of the 20 segments. For FBP, previously established cutoff values were used (1): SSS less than 4 was considered normal, 4–8 mildly abnormal, 9–13 moderately abnormal, and more than 13 severely abnormal. By contrast, no cutoff values have been established for CT-AC.

Follow-up

The following major adverse cardiac events (MACEs) were defined as endpoints: cardiac death and nonfatal myocardial infarction. For the analysis of any adverse cardiac events, hospitalizations for any cardiac reason, including unstable angina and coronary revascularization, were combined with MACEs.

Statistical Analysis

SPSS software (version 15.0; SPSS Inc.) was used for statistical testing. Quantitative variables were expressed as mean \pm SD and categorical variables as frequencies, mean, or percentages. A Wilcoxon signed rank test was used to compare mean values of SSSs. Patient groups were compared using 1-way ANOVA for continuous variables and an χ^2 test for categorical variables. Differ-

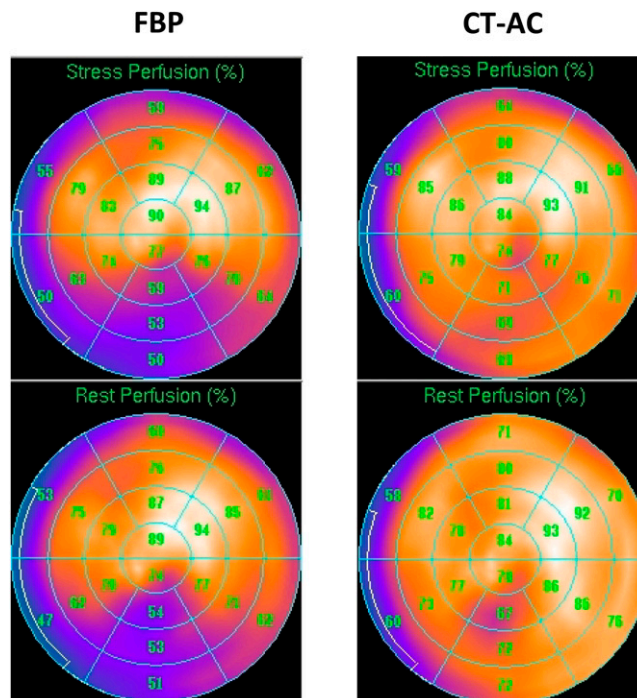


FIGURE 1. MPI polar map showing inferior attenuation artifact with FBP, which is resolved by applying CT-AC.

ences in survival over time were analyzed by the Kaplan–Meier method. The log-rank test was used to compare the survival curves. *P* values of less than 0.05 were considered statistically significant.

RESULTS

The baseline characteristics of the final population ($n = 876$) are presented in Table 1.

SSS in CT-AC and Noncorrected SPECT MPI

Mean (\pm SD) FBP SSS in all patients was 7.9 ± 5.9 , and mean CT-AC SSS was 5.9 ± 5.5 (decrease of 25.3%, $P < 0.001$). Of the 876 patients, 862 patients had an FBP SSS greater than 0 and 833 patients a CT-AC SSS greater than 0. An FBP SSS greater than 3 was present in 712 patients, and a CT-AC SSS greater than 3 was found in 533 patients.

Outcome

During a mean follow-up of 2.3 ± 0.6 y, a total of 184 adverse events occurred in 145 patients, including 35 MACEs, with 16 cardiac deaths (rate, 1.8%) and 19 nonfatal myocardial infarctions (rate, 2.2%). Notably, the MACE rate was significantly higher in patients with known CAD than in patients with suspected (but no known) CAD (7.3% vs. 1.5%, $P < 0.001$).

Figure 2 shows the MACE rates according to the SSS values (0, 1–3, 4–8, 9–13, and >13). With FBP, there was a marked increase in MACE rate from an SSS of 1–3 (0.7%; $n = 150$) to an SSS of 4–8 (4.3%; $n = 413$), with no further increase at an SSS of 9–13 (3.8%; $n = 199$). An SSS greater than 13 was identified as a cutoff indicating the high-risk group (MACE rate, 9.0%; $n = 100$). By contrast,

TABLE 1
Baseline Characteristics of Study Population (*n* = 876)

Characteristic	<i>n</i>
Male sex	558 (63.7)
Age (y)	65 ± 11
Body mass index (kg/m ²)	27.1 ± 4.9
Known CAD	343 (39.2)
Cardiovascular risk factors	
Hypertension	529 (60.4)
Dyslipidemia	360 (41.1)
Diabetes	165 (18.8)
Smoking	366 (41.8)
Positive family history	259 (29.6)

Data are mean ± SD or number, with percentages in parentheses.

with CT-AC the sharpest increase from low to intermediate MACE rate was observed at a lower SSS, namely between an SSS of 0 (0%; *n* = 43) and 1–3 (3.7%; *n* = 300), with a plateau at 4–8 (3.2%; *n* = 347). A further increase was seen at a CT-AC SSS of 9–13 (6.7%; *n* = 119) and greater than 13 (7.5%; *n* = 67). This increase yielded optimal cutoff values for a CT-AC SSS of 0, 1–8, and greater than 8 to describe low, intermediate, and high risk for MACEs (0%, 3.4%, and 7.0%, respectively; *P* < 0.01) and for all adverse events (2.3%, 18.2%, and 34.9%, respectively; *P* < 0.001). Figure 3 illustrates the survival free of MACEs (A) and free of any event (B) for the low-, intermediate-, and high-risk groups (i.e., CT-AC SSS 0, 1–8, and >8). Direct comparison of CT-AC and FBP of an SSS of 1–3 by a χ^2 test reached a *P* value of 0.05 for MACEs and a *P* value less than 0.01 for any cardiac events.

DISCUSSION

Our study is the first, to our knowledge, to assess the prognostic value of CT-AC for SPECT MPI. The present results demonstrate that CT-AC is helpful for risk stratification of SPECT MPI, adding incremental prognostic value.

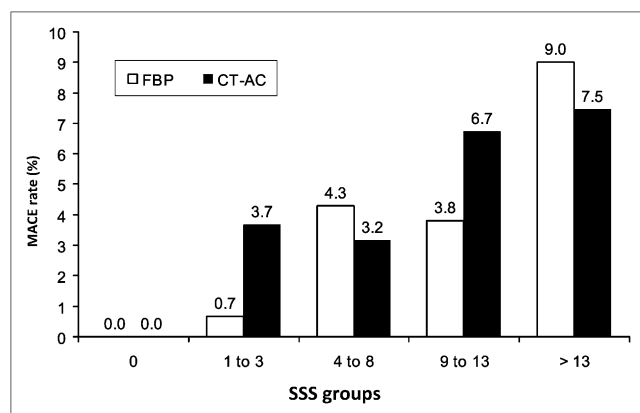


FIGURE 2. Rates of MACEs (cardiac death or myocardial infarction) are given for different ranges of SSS. With attenuation correction, prognostically relevant SSS cutoff is shifted toward lower values.

The relevant SSS cutoff value for predicting prognosis is shifted toward lower values when using CT-AC.

SPECT MPI is a well-established method for the evaluation of known or suspected CAD, and several studies have shown the strong prognostic value of SPECT MPI (1–3). Soft-tissue attenuation and subdiaphragmatic gastrointestinal activity play a major role in SPECT MPI because they can affect the diagnostic accuracy, mainly by decreasing specificity, and as a consequence reduce cost-effectiveness (21,22) or even lead to nondiagnostic studies (22). AC has provided higher left ventricular count homogeneity in healthy patients (9,12,23), facilitating interpretation of MPI studies and resulting in improved diagnostic accuracy (23,24). Therefore, several strategies for AC have been evaluated, among which CT-AC has proved most successful (9,25). Despite the fact that AC is increasingly used for SPECT MPI scans, there is a lack of data on the impact of CT-AC on the prognostic value of SPECT MPI. So far, only 2 studies have shown the prognostic value of AC in SPECT MPI (26,27). Both studies used an external gadolinium (¹⁵³Gd) line source for AC. Baghdasarian et al. demonstrated that AC provides powerful risk stratification when added to clinical variables in SPECT MPI in patients in whom ECG gating was not feasible because of arrhythmia (26). Our study extends this observation to x-ray-based AC and to an unselected patient population. CT-AC has the advantage of being more convenient in clinical practice than radioisotope transmission sources because they need replacement at regular intervals to maintain high-quality transmission maps, and cross-talk of ^{99m}Tc into the ¹⁵³Gd window has been shown to cause artifacts in patients with intense gastrointestinal uptake (9). Our results suggest a more homogeneous count distribution after CT-AC as the cutoff for SSS values indicating a high risk of events are shifted toward lower levels—clearly a result of a reduced number of false-positive scan results with CT-AC. The discrimination between true and false defects has been one of the major challenges in nuclear cardiology. Our results show that attenuation correction, especially with CT, successfully reduces the number of false-positive results. Although with standard FBP reconstruction patients with an SSS of 0–3 were considered at low risk, our results show that a CT-AC SSS of 1 or more already is associated with intermediate MACE risk. Moreover, the SSS cutoff value identifying high-risk patients is lower with than without CT-AC (CT-AC SSS > 8 vs. SSS > 13), implying that more attention has to be paid to smaller defects. Considering smaller defects more closely is necessary, in particular, because a CT-AC SSS of 0 is associated with no risk (0% MACE event rate) whereas the event rate in the traditionally “healthy” FBP SSS group of 0–3 was 0.6%, showing an improved risk stratification with CT-AC. The fact that smaller defects in AC images are associated with higher risk should also be considered in further patient management.

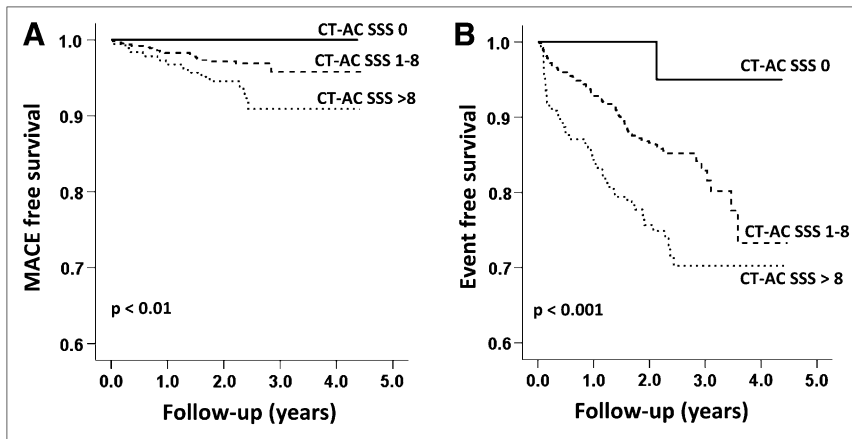


FIGURE 3. Kaplan–Meier survival curves for MACE-free and event-free survival.

The low event rate in patients with a CT-AC SSS of 0 was maintained over at least 4 y, perhaps suggesting a warranty period of more than 4 y for this low-risk population. By contrast, many events were observed in the intermediate-risk group (CT-AC SSS, 1–8) after 2.8 y, leading to a merging with the high-risk group (CT-AC SSS, >8) after 3.5 y (Fig. 3B). This merge may be interpreted as a process of atherosclerosis precipitating after 2.8 y, causing a shift toward the high-risk population.

We acknowledge the following limitations to our study. First, our data are based on a single-center study with a limited population. Further studies in larger populations may be helpful to study the prognostic value of CT-AC in different subgroups to assess the impact of sex and obesity. Second, because we included patients with follow-up information available in medical charts, the possibility cannot be excluded that the event rate for those patients lost to follow-up (17%) may have been different. On the other hand, because those patients with the largest findings at SPECT MPI were not deferred from treatment in our observational study, their risk of MACEs may be underestimated. Finally, the use of x-ray–based AC maps is associated with an additional radiation exposure.

CONCLUSION

The present study documented that CT-AC for SPECT MPI adds incremental prognostic value allowing improved risk stratification. Patients with a CT-AC SSS of 0 have an excellent prognosis, with a warranty period of at least 4 y. The prognostically relevant SSS cutoff is shifted toward lower values, which needs to be considered in patient management.

ACKNOWLEDGMENTS

We are grateful to Ennio Mueller, Edlira Loga, Mirjam De Bloeme, and Désirée Beutel for their excellent technical support. The study was supported by a grant from the Swiss National Science Foundation and from the Zurich Center for Integrative Human Physiology (ZIHP).

REFERENCES

- Hachamovitch R, Berman DS, Shaw LJ, et al. Incremental prognostic value of myocardial perfusion single photon emission computed tomography for the prediction of cardiac death: differential stratification for risk of cardiac death and myocardial infarction. *Circulation*. 1998;97:535–543.
- Gimelli A, Rossi G, Landi P, et al. Stress/rest myocardial perfusion abnormalities by gated SPECT: Still the best predictor of cardiac events in stable ischemic heart disease. *J Nucl Med*. 2009;50:546–553.
- Galassi AR, Azzarelli S, Tomaselli A, et al. Incremental prognostic value of technetium-99m-tetrofosmin exercise myocardial perfusion imaging for predicting outcomes in patients with suspected or known coronary artery disease. *Am J Cardiol*. 2001;88:101–106.
- Fleischmann S, Koepfli P, Namdar M, Wyss CA, Jenni R, Kaufmann PA. Gated ^{99m}Tc-tetrofosmin SPECT for discriminating infarct from artifact in fixed myocardial perfusion defects. *J Nucl Med*. 2004;45:754–759.
- DePuey EG, Rozanski A. Using gated technetium-99m-sestamibi SPECT to characterize fixed myocardial defects as infarct or artifact. *J Nucl Med*. 1995; 36:952–955.
- Segall GM, Davis MJ. Prone versus supine thallium myocardial SPECT: a method to decrease artifactual inferior wall defects. *J Nucl Med*. 1989;30:548–555.
- Tan P, Bailey DL, Meikle SR, Eberl S, Fulton RR, Hutton BF. A scanning line source for simultaneous emission and transmission measurements in SPECT. *J Nucl Med*. 1993;34:1752–1760.
- Schepis T, Gaemperli O, Koepfli P, et al. Use of coronary calcium score scans from stand-alone multislice computed tomography for attenuation correction of myocardial perfusion SPECT. *Eur J Nucl Med Mol Imaging*. 2007;34:11–19.
- Masood Y, Liu YH, Depuey G, et al. Clinical validation of SPECT attenuation correction using x-ray computed tomography-derived attenuation maps: multicenter clinical trial with angiographic correlation. *J Nucl Cardiol*. 2005;12:676–686.
- Duvernoy CS, Ficaro EP, Karabajakian MZ, Rose PA, Corbett JR. Improved detection of left main coronary artery disease with attenuation-corrected SPECT. *J Nucl Cardiol*. 2000;7:639–648.
- Hoefflinghaus T, Husmann L, Valenta I, et al. Role of attenuation correction to discriminate defects caused by left bundle branch block versus coronary stenosis in single photon emission computed tomography myocardial perfusion imaging. *Clin Nucl Med*. 2008;33:748–751.
- Ficaro EP, Fessler JA, Shreve PD, Kritzman JN, Rose PA, Corbett JR. Simultaneous transmission/emission myocardial perfusion tomography: diagnostic accuracy of attenuation-corrected ^{99m}Tc-sestamibi single-photon emission computed tomography. *Circulation*. 1996;93:463–473.
- Malkerneker D, Brenner R, Martin WH, et al. CT-based attenuation correction versus prone imaging to decrease equivocal interpretations of rest/stress Tc-99m tetrofosmin SPECT MPI. *J Nucl Cardiol*. 2007;14:314–323.
- Koepfli P, Hany TF, Wyss CA, et al. CT attenuation correction for myocardial perfusion quantification using a PET/CT hybrid scanner. *J Nucl Med*. 2004;45: 537–542.
- O'Connor MK, Kemp BJ. Single-photon emission computed tomography/computed tomography: basic instrumentation and innovations. *Semin Nucl Med*. 2006;36:258–266.
- Heller GV, Links J, Bateman TM, et al. American Society of Nuclear Cardiology and Society of Nuclear Medicine joint position statement: attenuation

- correction of myocardial perfusion SPECT scintigraphy. *J Nucl Cardiol.* 2004; 11:229–230.
17. Burkhard N, Herzog BA, Husmann L, et al. Coronary calcium score scans for attenuation correction of quantitative PET/CT ¹³N-ammonia myocardial perfusion imaging. *Eur J Nucl Med Mol Imaging.* 2010;37:517–521.
 18. Hansen CL, Goldstein RA, Akinboboye OO, et al. Myocardial perfusion and function: single photon emission computed tomography. *J Nucl Cardiol.* 2007; 14:e39–e60.
 19. Berman DS, Kang X, Van Train KF, et al. Comparative prognostic value of automatic quantitative analysis versus semiquantitative visual analysis of exercise myocardial perfusion single-photon emission computed tomography. *J Am Coll Cardiol.* 1998;32:1987–1995.
 20. Hesse B, Tagil K, Cuocolo A, et al. EANM/ESC procedural guidelines for myocardial perfusion imaging in nuclear cardiology. *Eur J Nucl Med Mol Imaging.* 2005;32:855–897.
 21. Fleischmann KE, Hunink MG, Kuntz KM, Douglas PS. Exercise echocardiography or exercise SPECT imaging? A meta-analysis of diagnostic test performance. *JAMA.* 1998;280:913–920.
 22. Kuntz KM, Fleischmann KE, Hunink MG, Douglas PS. Cost-effectiveness of diagnostic strategies for patients with chest pain. *Ann Intern Med.* 1999;130:709–718.
 23. Grossman GB, Garcia EV, Bateman TM, et al. Quantitative Tc-99m sestamibi attenuation-corrected SPECT: development and multicenter trial validation of myocardial perfusion stress gender-independent normal database in an obese population. *J Nucl Cardiol.* 2004;11:263–272.
 24. Heller GV, Bateman TM, Johnson LL, et al. Clinical value of attenuation correction in stress-only Tc-99m sestamibi SPECT imaging. *J Nucl Cardiol.* 2004;11:273–281.
 25. Fricke E, Fricke H, Weise R, et al. Attenuation correction of myocardial SPECT perfusion images with low-dose CT: evaluation of the method by comparison with perfusion PET. *J Nucl Med.* 2005;46:736–744.
 26. Baghdasarian SB, Noble GL, Ahlberg AW, Katten D, Heller GV. Risk stratification with attenuation corrected stress Tc-99m sestamibi SPECT myocardial perfusion imaging in the absence of ECG-gating due to arrhythmias. *J Nucl Cardiol.* 2009;16:533–539.
 27. Gibson PB, Demus D, Noto R, Hudson W, Johnson LL. Low event rate for stress-only perfusion imaging in patients evaluated for chest pain. *J Am Coll Cardiol.* 2002;39:999–1004.